Int. J. Electrochem. Sci., 11 **(2016)** 1868 - 1882

International Journal of
ELECTROCHEMICAL
SCIENCE
www.electrochemsci.org

Corrosion Performance of Ni-Based Alloys in Sodium Metavanadate

O. Sotelo-Mazon[1,2], *J. Porcayo-Calderon*[1,*], *C. Cuevas-Arteaga*[1], *G. Salinas-Solano*[1], *J.J. Ramos-Hernandez*[1,3], *E. Vazquez-Velez*[2], *L. Martinez-Gomez*[2,4]

[1]Universidad Autonoma del Estado de Morelos, CIICAp, Avenida Universidad 1001, 62209 Cuernavaca, MOR, Mexico
[2]Instituto de Ciencias Fisicas, Universidad Nacional Autonoma de Mexico, Avenida Universidad s/n, 62210 Cuernavaca, MOR, Mexico
[3]Facultad de Quımica, Universidad Nacional Autonoma de Mexico, 04510 Mexico, DF, Mexico
[4]Corrosion y Proteccion, Buffon 46, 11590 Mexico, D.F., Mexico
[*]E-mail: jporcayoc@gmail.com

Received: 18 November 2015 / *Accepted:* 17 December 2015 / *Published:* 1 February 2016

Hot corrosion or molten salt corrosion is a form of corrosion which consumes materials to high corrosion rates, because it destroys the protective oxide layer formed on the metal surface. Therefore, it has been developed more resistant materials such as superalloys which have been manufactured for high temperature applications. A study of the corrosion performance of Ni-based alloys (Inconel 600, 601, 617 and 625) in $NaVO_3$ molten salt at 700 °C was realized. In order to determine the corrosion resistance of the alloys, electrochemical techniques and weight loss tests were used. Electrochemical techniques applied were polarization potentiodynamic curves, open circuit potential and the linear polarization resistance. Analyses were conducted by scanning electron microscopy and X-ray diffraction to analyze the products of corrosion. It was observed that Inconel 600 and 601 showed the best corrosion resistance, however the Inconel 617 and 625 showed a low performance. It is known that Cr is responsible for the corrosion resistance; this due to the formation of the protective layer of Cr_2O_3, however, the Ni content plays an important role in the performance of this type of materials, as well as the other alloying elements (Al, Ti, Nd, Co and Mo).

Keywords: Superalloys, molten salts, vanadates, hot corrosion, electrochemical techniques

1. INTRODUCTION

Corrosion is a degradation process due to the interaction between a material and the environment where it is immersed. This degradation process affects the physical, chemical and mechanical properties of the materials [1]. Due to the reduction of high grade fuel and for economic reasons, the use of residual fuel oil was amply utilized, especially in power generation systems. The ashes formed during the combustion process of residual fuel oil contain high concentrations of the elements vanadium, sodium and sulfur, which form some compounds such as Na_2SO_4 and V_2O_5, and some other complex compounds called sodium vanadyl vanadates [2-5]. Sodium vanadyl vanadates are present as $NaVO_3$ (meta-vanadate), $Na_2S_2O_7$ (sodium pyro-sulfate), $Na_2O{\cdot}V_2O_4{\cdot}5V_2O_5$ (beta vanadyl vanadate) and $5Na_2O{\cdot}V_2O_4{\cdot}11V_2O_5$ (gama vanadil vanadate) among others [5-6]. Vanadium compounds are very stable and corrosive under normal operation conditions of power station boilers [5-8]. Iron base alloys and nickel base superalloys are very common commercial alloys used for high temperature applications, for instance, in the manufacture of components used for aggressive environmental of gas turbine and vapor generators. Alloys used to manufacture components such as turbine blades must have excellent mechanical performance and corrosion resistance [10].

In this paper, the corrosion resistance of Ni-based alloys (Inconel 600, 601, 617 and 625) in $NaVO_3$ molten salt at 700 °C was evaluated. Electrochemical techniques such as linear polarization resistance and polarizations curves were applied, together with the measurement of the free corrosion potential. Weight loss method was also applied, making a comparison between the electrochemical and the conventional results.

2. MATERIALS AND METHODS

Chemical composition of the Ni-based alloys (Inconel 600, 601, 617 and 625) is presented in table 1. Samples from these alloys were cut as small parallelepipeds sized 10 × 5 × 5 mm. In order to obtain a defined area and a homogeneous surface, the samples were grinded with silicon carbide paper 600 grit, washed with distilled water, and degreased with acetone before the corrosion tests.

Table 1. Chemical composition of the Ni-based alloys.

	Composition [% weight]									
Alloy	Cr	Ni	Fe	Al	Mo	Co	Nd	Ti	Cu	C
Inconel 600	15.5	76.0	8.0	---	---	---	---	---	0.25	0.08
Inconel 601	23.0	60.5	14.1	1.35	---	---	---	---	0.5	0.05
Inconel 617	22.0	55.0	---	1.0	9.0	12.5	---	---	---	0.07
Inconel 625	21.5	61.0	2.5	0.2	9.0	---	3.6	0.2	---	0.05

For the weight loss tests, four specimens of each alloy and measuring point were used. Three were used to determine the mass loss, and the fourth was encapsulated and analyze it in cross section. Prior to the corrosion tests, the metal coupons were degreased with acetone, dried and then they were measured and weighed to determine their reaction area and mass. Each specimen was packed in the corrosive salt in alumina crucibles with 500 mg/cm^2 of $NaVO_3$. In this condition the specimens were introduced in an electric furnace at 700 °C in static air. Each 48 hours, four specimens were removed from the furnace until complete 248 hours. For each experimental condition, three corroded samples were cleaned according to standard ASTM G1, a fourth specimen was mounted in resin and it was polished in cross section to analyze the corrosive attack.

For electrochemical measurements, a Ni20Cr wire was spot welded to the specimens (working electrode). The Ni20Cr wire was isolated with an alumina tube and the gap between the ceramic tube and the Ni20Cr wire was filled with refractory cement. The reference electrode and counter electrode were platinum wires with 0.5 mm diameter. Platinum electrode was used in previous studies, and it has been shown that it can be used as reference electrode [7, 11-12].

One of the main problems concerning the application of electrochemical techniques in the study of molten salt corrosion is the correct choice of the reference electrode. However, many studies support the use of platinum immersed directly into the molten salt as an excellent option to be used as reference electrode [13-23]. Even though the redox electrochemical couple has been not identified and reported. Kasen and Jones [24] indicate that where the usual reference electrodes such as calomel or Ag/AgCl/KCl electrodes cannot be used (high temperatures, molten electrolytes), Pt is the reference electrode of choice.

Electrochemical tests were performed using a potentiostat-galvanostat ACM Instruments. The reported potentials are with reference to the platinum electrode. The corrosive salt ($NaVO_3$) was contained in an alumina crucible, and placed inside an electric tube furnace. When the test temperature was reached (700 °C), the three-electrodes arrangement was introduced to the molten salt. The atmosphere above the melt was static air. Before starting the electrochemical measurements, the electrochemical cell was held during 30 minutes until the stable state was reached.

In order to determine the corrosion resistance of the Ni-based alloys, potentiodynamic polarization curves (PC), open circuit potential (OCP), and linear polarization resistance (LPR) were obtained. PC measurements were carried out applying an overpotential from 400 mV to 1500 mV with respect to the corrosion potential (Ecorr) at a scan rate of 1 mV/s. Electrochemical parameters such as Tafel slopes, Ecorr and Icorr, were obtained from the anodic and cathodic regions of the polarization curves. LPR measurements were obtained each 4 hours applying an overpotential of ± 20 mV with respect to the Ecorr at a scan rate of 1 mV/s. The open circuit potential was taken using a platinum wire as the reference electrode. The corroded specimens were mounted in thermosetting resin and analyzed by scanning electron microscopy (Zeiss DSM Karl-950).

3. RESULTS AND DISCUSSION

3.1. Weight Loss Method Results

The weight loss measurements of the Ni-based alloys are presented in Figure 1. Weight loss method gives a cumulative measure of the corrosion rate. In this case, it is observed that during the first 100 hours the Inconel 600, 601 and 625 increase their weight loss abruptly, and after the weight loss values are practically constant with a slight increase until the end of the test. On the contrary, the Inconel 617 showed a continuous increase in the weight loss values throughout the corrosion test.

Corrosion resistance shown by the different materials is related to its chemical composition, mainly with its chromium content. Chromium is the element responsible for the formation of the protective oxide. In this sense, it can be observed that Inconel 601 has the highest chromium content (23%) and this alloy had the greatest corrosion resistance, followed by Inconel 600 (15.5% Cr). Clearly, increasing the chromium content (7.5%) favored an increase in the corrosion resistance of the Inconel 601. However, the behavior shown by Inconel 617 and Inconel 625 was different, that is, even though both have similar chromium content that Inconel 601, the corrosion rate was higher than that of Inconel 600. In this case, it can be inferred that the poor performance of Inconel 625 can be due to its high Mo content. Similarly, the poor performance observed for Inconel 617 is due to its Mo content and by the presence of Co. Both alloys have the same Mo content, similar Cr content, but the main difference is the presence of Co, this suggests that the presence of both Co and Mo provoked the biggest degradation of Inconel 617. Although the corrosion resistance of these alloys is based on the growth of a protective layer of Cr_2O_3, the continuous dissolution of the protective oxide leads to the formation of other oxides of the various elements of the alloy, for example, NiO, Fe_2O_3, Al_2O_3, MoO_3, CoO. The presence of different types of metallic oxides can promote a synergistic dissolution process increasing the corrosion rate of the alloy. In this case, some metallic oxides undergo an acid dissolution process and other metallic oxides a basic dissolution process. This will cause changes in the basicity of melt increasing the dissolution rate the metallic oxides. In some cases once the salt film is saturated with corrosion products, and the basicity of the melt is stabilized at a value where the different oxides have approximately equal solubility, the sustained hot corrosion of the alloys does not continue [25].

Figure 2 presents the micrographs of corroded specimens exposed to the $NaVO_3$ molten salt during 248 hours. In the case of Inconel 600 and 601 a generalized corrosion process throughout the surface seems to be observed, however a significant amount of local attack and intergranular corrosion process are present. The local attack is in form of severe pitting, observing around the pits the cathodic areas. Pitting corrosion phenomenon is that in which the material is passivated, and suffers a disruption of the passive film, causing the appearance of active areas with high corrosion rates [26]. By contrast, the surface appearance of Inconel 617 corresponds to a generalized corrosion process. On the other hand, surface appearance showed by Inconel 625 exhibited a generalized corrosion process besides the presence of large voids possibly generated by the detachment of the Nd-rich precipitates of the alloy. These precipitates generated anodic-cathodic sites which favored the corrosion of the alloy, and eventually caused the detachment of the Nd-rich precipitates.

Figure 3 shows a micrograph of a cross section of the metal-scale interface of the corroded sample of Inconel 600 exposed to $NaVO_3$ molten salt at 700 °C during 248 hours. Also X-ray mapping elements are presented. It is observed a thick layer of corrosion products and according to the mapping of elements; the outer area is rich in Cr and O, possibly Cr_2O_3 reprecipitated after being dissolved by $NaVO_3$. The remainder of the corrosion products layer is rich in Fe, Cr, Ni, O and V. This indicates that the alloy was not able to develop a protective layer and underwent a continuous corrosion process. This could have happened in the first 100 hours of testing. Subsequently, the thickness of the corrosion product layer prevented the $NaVO_3$ diffusion generating a decrease in corrosion rate.

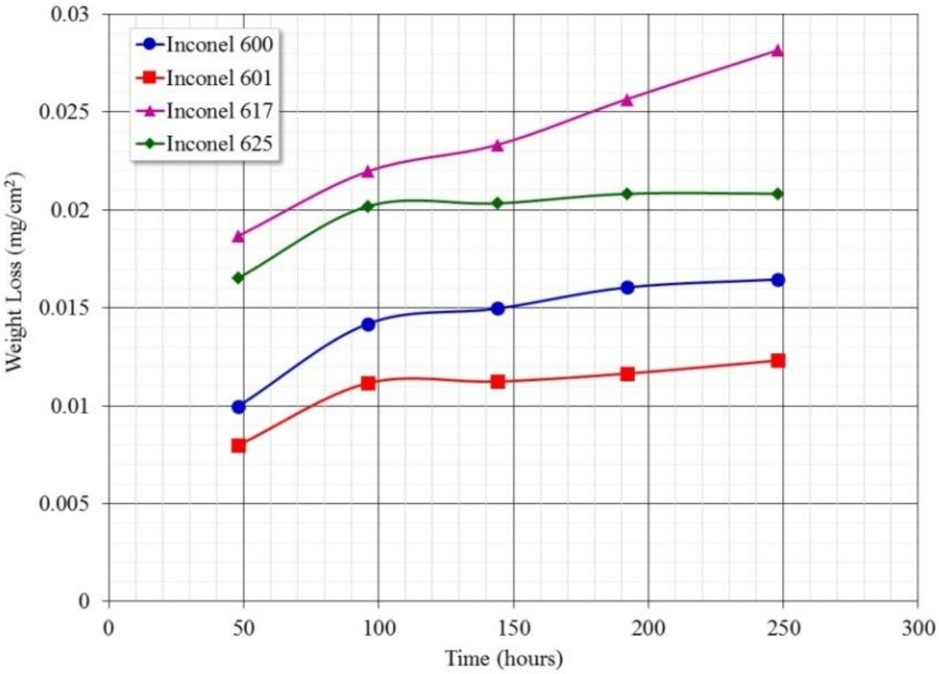

Figure 1. Weight loss for Ni-base alloys exposed to $NaVO_3$ at 700°C in static air.

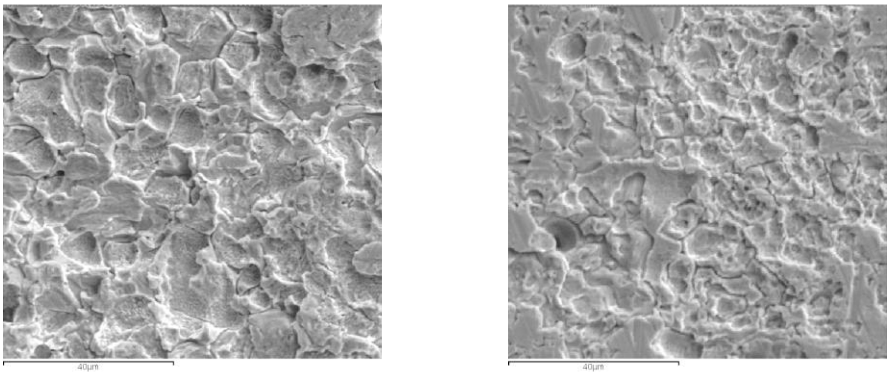

Inconel 600 Inconel 601

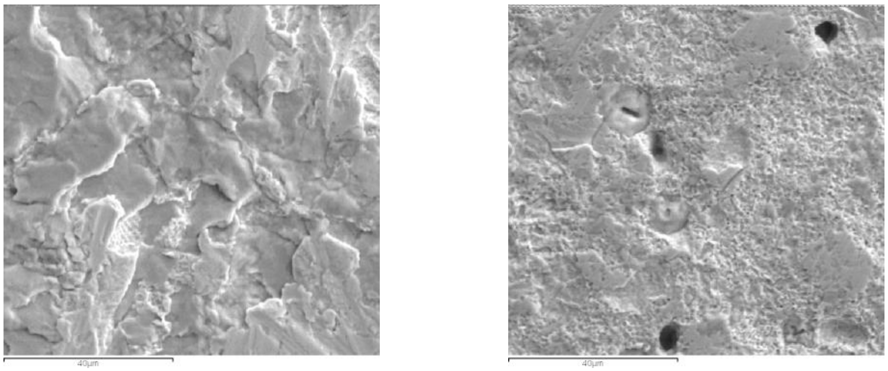

Inconel 617 Inconel 625

Figure 2. Superficial micrographs of the clean materials after exposed to $NaVO_3$ for 248 hours at 700 °C.

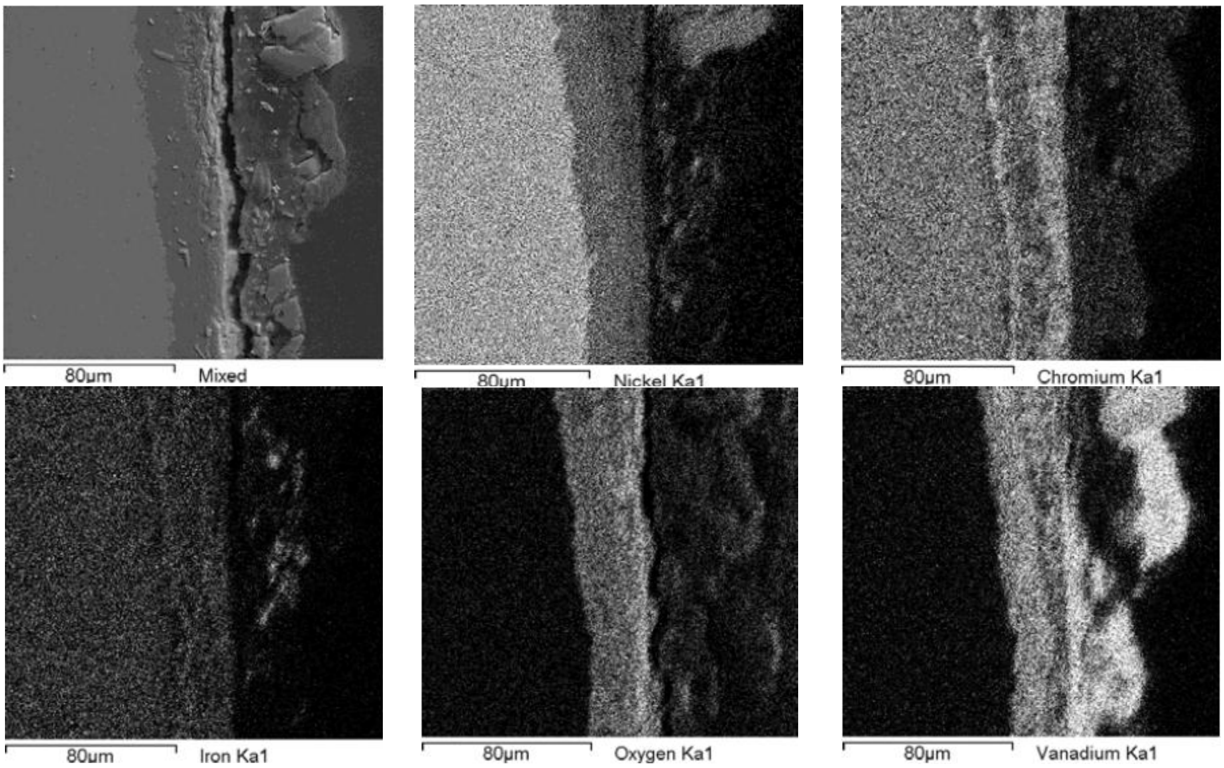

Figure 3. Micrograph of Inconel 600 corroded in $NaVO_3$ for 248 hours at 700 °C together with X-ray mappings of Fe, Cr, Ni, O and V.

Figure 4 shows a micrograph of a cross section of the metal-scale interface of the corroded sample of Inconel 601 exposed to $NaVO_3$ molten salt at 700 °C during 248 hours. Also X-ray mapping elements are presented. According to the elements mapping in the corrosion products-alloy interface is observed a discontinuous layer rich in Cr and O, which may correspond to Cr_2O_3. Onto the surface alloy both Cr-depletion and Ni-enrichment is observed. These characteristics are typical of alloys undergoing a continuous dissolution process of the protective oxide [27-29]. Onto this layer the presence of Cr, Ni, Fe, O and V, possibly as metallic vanadates, are observed. The highest degradation rate was observed in the first 100 hours of testing. The highest corrosion resistance shown by this alloy was possibly due to the presence of the discontinuous layer of Cr_2O_3 onto the surface of the alloy.

Figure 5 shows a micrograph of a cross section of the metal-scale interface of the corroded sample of Inconel 617 exposed to $NaVO_3$ molten salt at 700 °C during 248 hours. Also X-ray mapping elements are presented. Onto the alloy surface a thick scale of corrosion products is observed, and this scale consists of different layers. According to the mapping of elements, the outer zone is formed by a thick layer rich in Ni, V and O, possibly as nickel vanadate. Subsequently, a thin layer rich in Cr, Co, V and O is observed, possibly as both oxides and vanadates metallic. Under these a layer rich in Ni, V and O, possibly as nickel vanadate, is observed. Finally, adhered onto alloy surface a thick layer rich in Cr, Co, V and O is observed, possibly as both oxides and vanadates metallic. The presence of Mo and Al is observed spread over the entire scale corrosion products. Inconel 617 has a similar Cr content to that of Inconel 601, however onto alloy surface does is not visible a significant Cr-depletion or a Ni-enrichment zone. This indicates that the alloy was not able to develop a protective Cr_2O_3 layer. This was because the alloy experienced continuous corrosion process, possibly due to the synergistic dissolution of the different metallic oxides formed [25, 30-31]. Because of this, the Inconel 617 showed the highest corrosion rate and a tendency to decreases during the 248 hours of immersion in $NaVO_3$ molten was not observed.

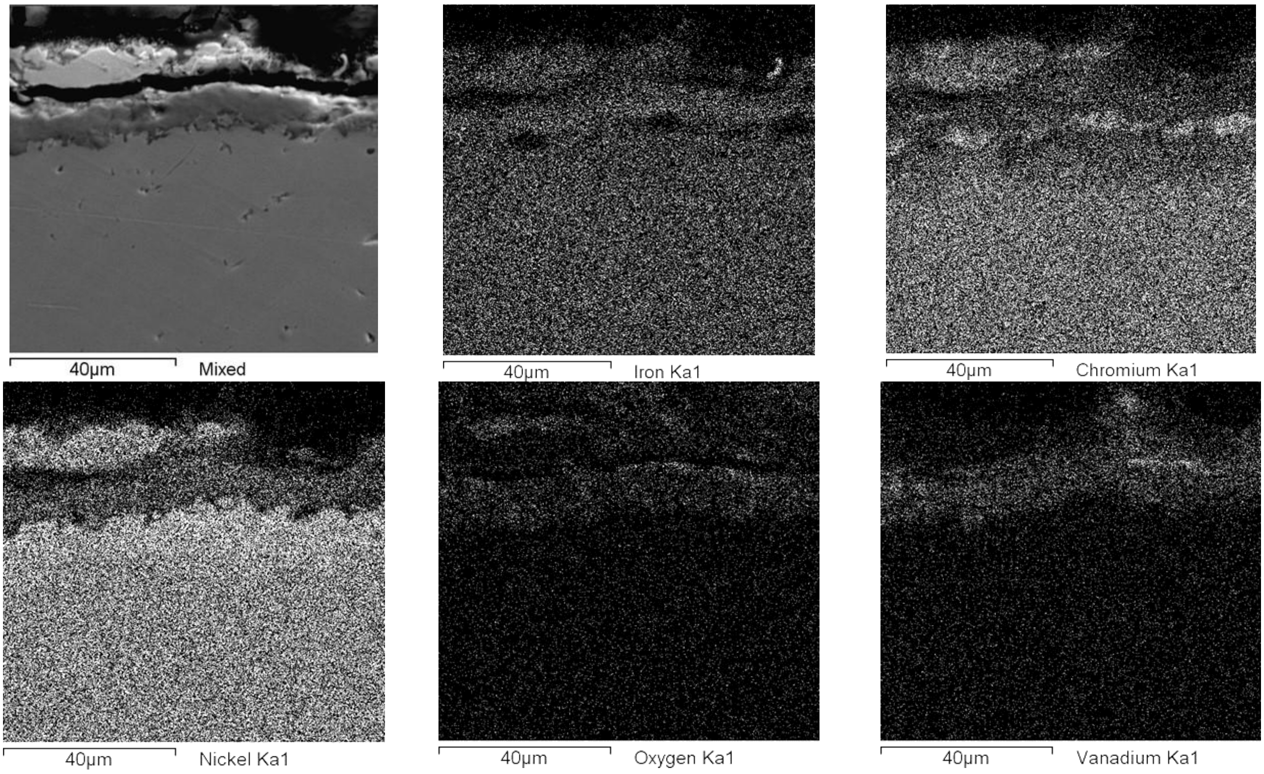

Figure 4. Micrograph of Inconel 601 corroded in $NaVO_3$ for 248 hours at 700°C together with X-ray mappings of Fe, Cr, Ni, O and V.

Figure 6 shows a micrograph of a cross section of the metal-scale interface of the corroded sample of Inconel 625 exposed to $NaVO_3$ molten salt at 700 °C during 248 hours. Also X-ray mapping elements are presented. From figure, a thick corrosion products scale is observed. Adhered to the alloy surface a high V concentration associated with the metallic elements of the alloy, possibly as metal vanadates, is observed. Adhered onto this layer, a thick layer rich in metallic elements and V, possibly both as oxides and vanadates, is also observed. The presence of Mo and Al is observed distributed into the corrosion products scale. Likewise, in the alloy surface both a significant Cr-depletion and Ni enrichment was not visible. This indicates that the alloy was not able to develop a protective Cr_2O_3 layer. The alloy also experienced a continuous corrosion process, possibly due to synergistic dissolution of the different metallic oxides formed [25, 30-31].

From the weight loss corrosion tests can be established that the corrosion resistance of the Ni-based alloys is in the following order; Inconel 601 > Inconel 600 > Inconel 625 > Inconel 617. It is important to note that the content of Mo and Co, and the presence of both Nd-rich and Ti-rich precipitates, influenced the low corrosion resistance of the Inconel 625 and Inconel 617.

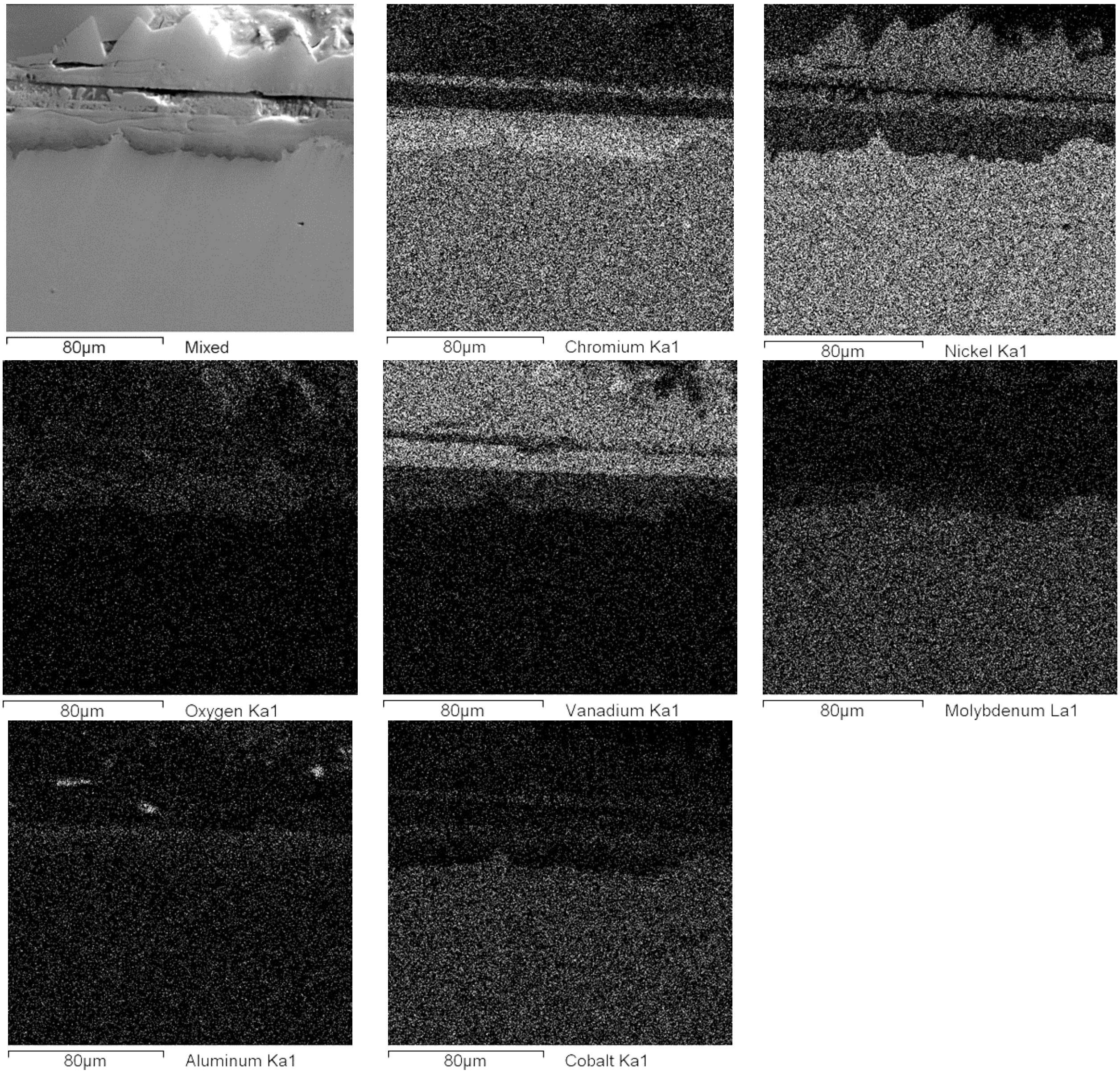

Figure 5. Micrograph of Inconel 617 corroded in $NaVO_3$ for 248 hours at 700 °C together with X-ray mappings of Cr, Ni, O, V, Al, Mo and Co.

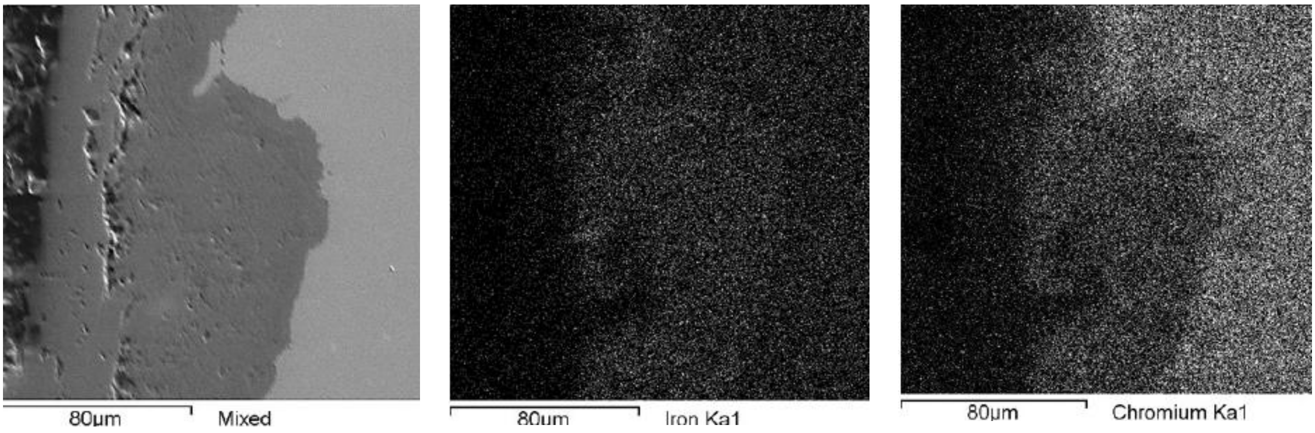

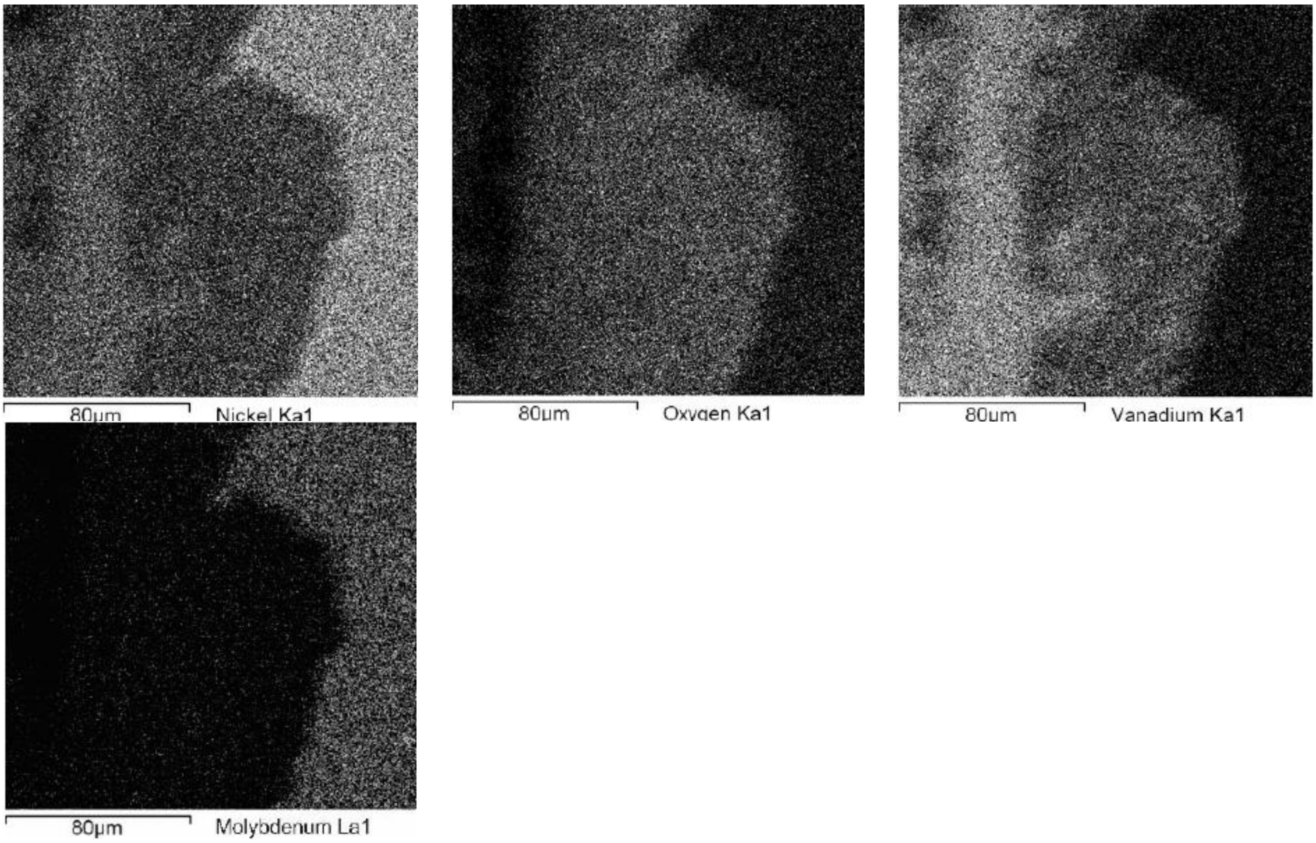

Figure 6. Micrograph of Inconel 625 corroded in $NaVO_3$ for 248 hours at 700°C together with X-ray mappings of Fe, Cr, Ni, O, V, Al, Mo and Nb.

3.2. Electrochemical Results

Figure 7 shows the potentiodynamic polarization curves obtained of the alloys evaluated in sodium metavanadate ($NaVO_3$), at 700 °C in static air at a scan rate of 1 mV/s. Polarization curves show that all materials tested exhibits an active corrosion behavior, and at anodic potentials does not reaches a passive behavior. Therefore, these alloys are susceptible to exhibit a continuous dissolution process of their protective oxides, as it was observed in the weight loss tests. In Table 2, the electrochemical parameters from the polarization curves are presented for the studied alloys. It is observed that Inconel 600 showed the highest corrosion rate (Icorr = 3.13 mA/cm^2), and Inconel 601 and Inconel 617 the lowest corrosion rate (≈ 0.9 mA/cm2). On the other hand, Inconel 625 exhibits the most active behavior (Ecorr = -260 mV), and Inconel 600 and 617 noblest behaviors (Ecorr ≈ -100 mV). From the potentiodynamic polarization curves can be established that the corrosion resistance of the Ni based alloys is in the following order; Inconel 601 ≈ Inconel 617 > Inconel 625 > Inconel 600. However, it is important to point out that potentiodynamic polarization curves just indicate a short term behavior (just when the corrosive system reaches the stable state). For greater immersion time, the behavior may be different because the chemical composition of the electrolyte can be altered (by the dissolution of the corrosion products, or depletion of one of the reactants), or because the material may be able to form more stable protective oxides [28-29]. It is for this reason, that the trends of corrosion resistance of the alloys are different to those observed in the weight loss test.

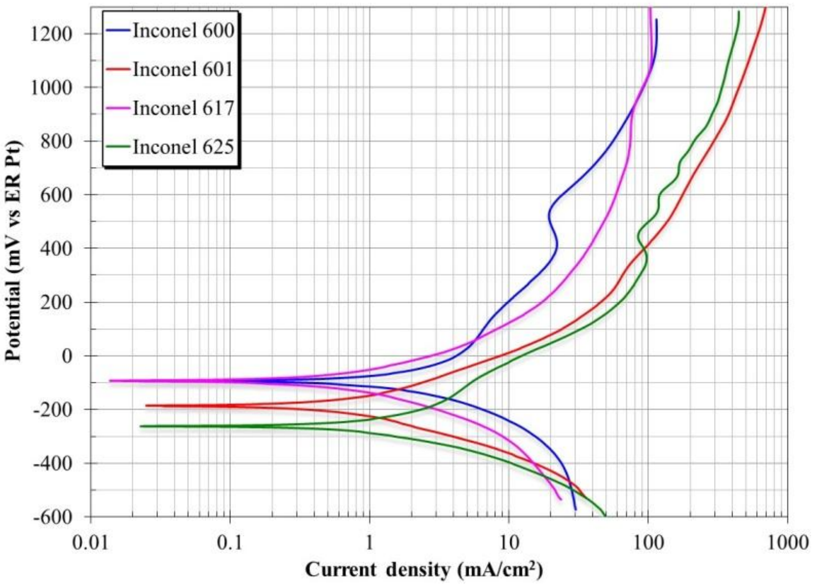

Figure 7. Potentiodynamic polarization curves of the Ni-based alloys in $NaVO_3$ at 700 °C in static air.

Table 2. Electrochemical parameters from potentiodynamic polarization curves for Ni-based alloys.

Materials	*E*corr (mV)	*Icorr* (mA/cm^2)	b_a	b_c
Inconel 600	-98	3.13	273	167
Inconel 601	-185	0.84	190	173
Inconel 617	-95	0.9	186	192
Inconel 625	-260	1.59	273	167

Because the trend of the Ecorr values of a material during the corrosive process states the condition or changes of the metallic oxides, and due that the protective layer plays an important role in the corrosion resistance of the materials, the Ecorr measurements are quiet significant. It is known that an increase in the Ecorr values usually indicates the formation of protective films; a stable Ecorr values indicate that the passive film is protective, and a decrease in the Ecorr values indicate the broken and dissolution or no formation of a protective film [32]. The ability of the materials to achieve a passive state depends of several processes such as the formation rate of a protective oxide, the ionic transport across oxide and the dissolution rate of the protective oxide [33]. Figure 8 shows the variation of the corrosion potential of Ni-based alloys measured during 100 hr. From figure, Inconel 600 shows a sharp drop in the Ecorr values in the first few hours of immersion, which indicates that the alloy was not able to form a passive layer in order to self-protect from the corrosive medium. After this, a steady increase in the Ecorr values is observed. This was possibly due to the formation of a corrosion product scale thus limiting the diffusion of the corrosive agent to the alloy surface. On the other hand, the other alloys exhibited a sharp increase in the Ecorr values in the first few hours of immersion, which indicates that the three alloys tended to form a passive layer to protect them from the corrosive medium. After that, in the case of Inconel 617, a steady increase in the Ecorr values is observed similar to the Ecorr values of Inconel 600. Inconel 601 and 625, also showed an increase in their Ecorr values, but with visible fluctuations. This indicates that these materials exhibit a continuous active-passive behavior.

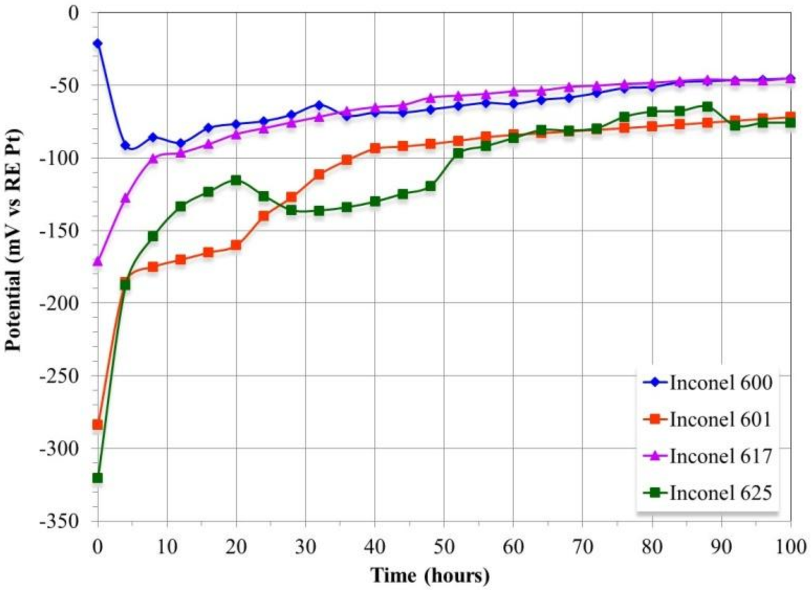

Figure 8. Corrosion potential of the Ni-based alloys exposed to $NaVO_3$ at 700°C in static air.

Figure 9 shows the variation of the corrosion rate (Icorr) of the Ni-based alloys evaluated in $NaVO_3$ at 700 °C for 100 hours. These results were obtained from the LPR measurements where the Icorr values were calculated using the Stern-Geary equation [34].

$$I_{corr} = \frac{b_a b_c}{2.303 R_p (b_a + b_c)}$$

Rp is the polarization resistance; ba and bc are the anodic and cathodic Tafel slopes reported in Table 2.

Inconel 600 presented the highest initial values of Icorr (7.3 mA/cm^2); subsequently until the 5 hours, it decreased rapidly to 0.5 mA/cm^2; after that, until the end of the test, Icorr kept decreasing lightly reaching the value of 0.3 mA/cm^2. It is probable that, the corrosion product scale limited the diffusion of the corrosive agent and enhanced the corrosion resistance of the alloy. Inconel 601 shows a decrease in the Icorr values during the first 5 hours of immersion (2.5 to 1.3 mA/cm^2) when the passive layer was formed. After that, the Icorr values tended to decrease during the rest of the exposure time to 1.1 mA/cm^2. Regarding Inconel 617 and 625, both materials showed a marked decrease in the Icorr values in the first 5 hours of immersion, after this, Icorr values tended to increase steadily during the rest of the immersion test. This indicates that initially the alloys tended to protect their protectors but were constantly oxides dissolved in the corrosive medium. This indicates that initially the alloys formed a protective oxide, but it was continuously dissolved in the corrosive medium [35].

Figure 10 shows the cross section of the metal-scale interface of the Ni-based alloys corroded in $NaVO_3$ molten salt at 700 °C during 100 hours. Also X-ray mapping elements of Cr and V are presented. It can be seen that the alloys do not show the presence of a protective chromium oxide film. This indicates that these alloys are susceptible to hot corrosion by vanadium salts. Furthermore, it is noteworthy that only the Inconel 600 and Inconel 601 are those with a thick layer of corrosion products adhered to its surface. Conversely, onto Inconel 617 surface is not observed a corrosion product layer. The permanence of a corrosion products layer may decreases the corrosion rate because hinders the diffusion of aggressive ions toward the metal surface.

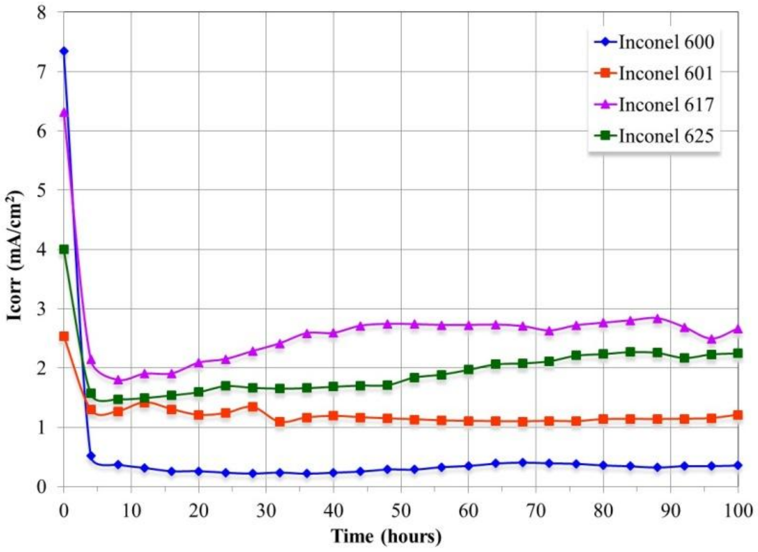

Figure 9. Current density corrosion (Icorr) for the Ni-based alloys exposed to $NaVO_3$ a 700°C in static air.

From the LPR measurements can be established that the corrosion resistance of the Ni-based alloys is in the following order; Inconel 600 > Inconel 601 > Inconel 625 > Inconel 617. Results are similar to those of the weight loss corrosion tests. Again the content of Mo and Co, and the presence of precipitates both Nd-rich and Ti-rich, influenced the low corrosion resistance of the Inconel 625 and Inconel 617.

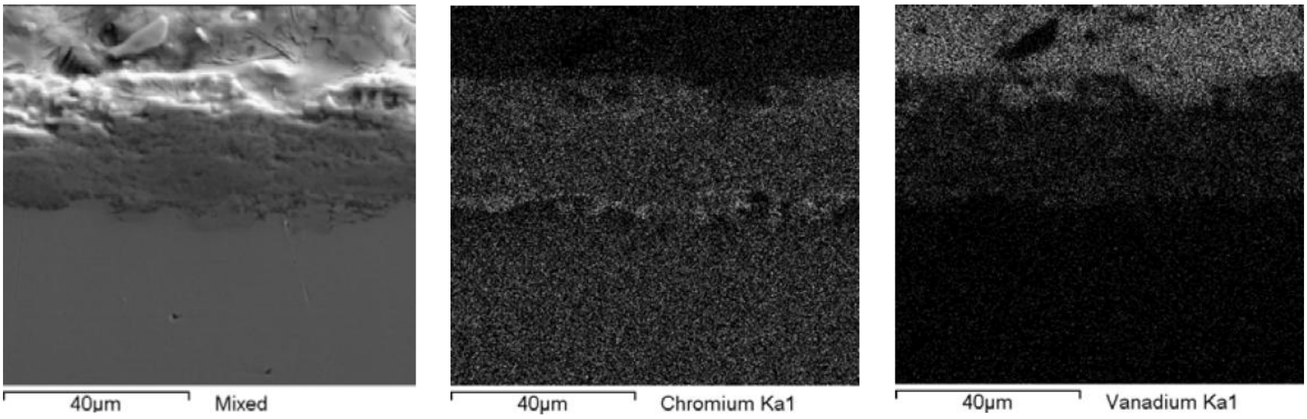

Inconel 600

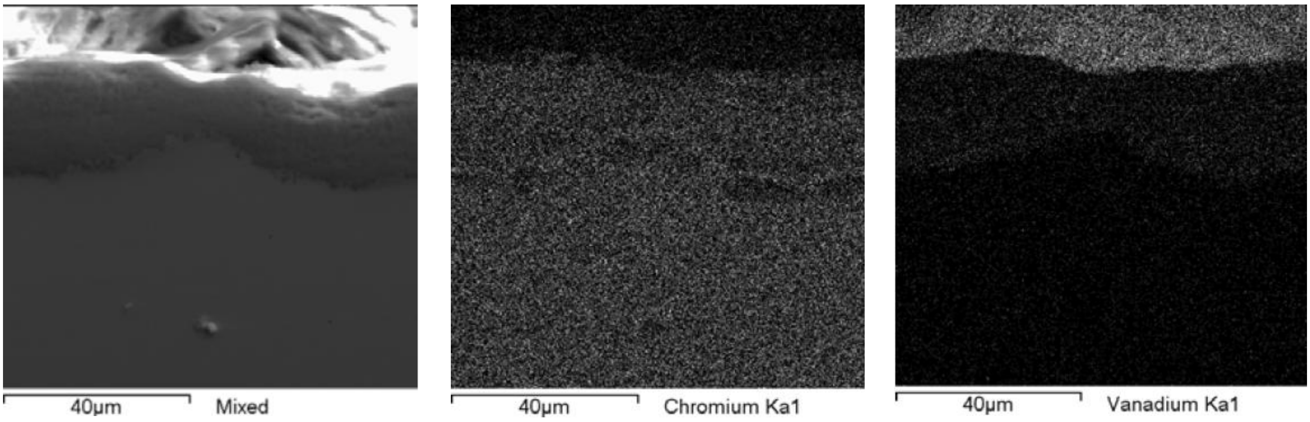

Inconel 601

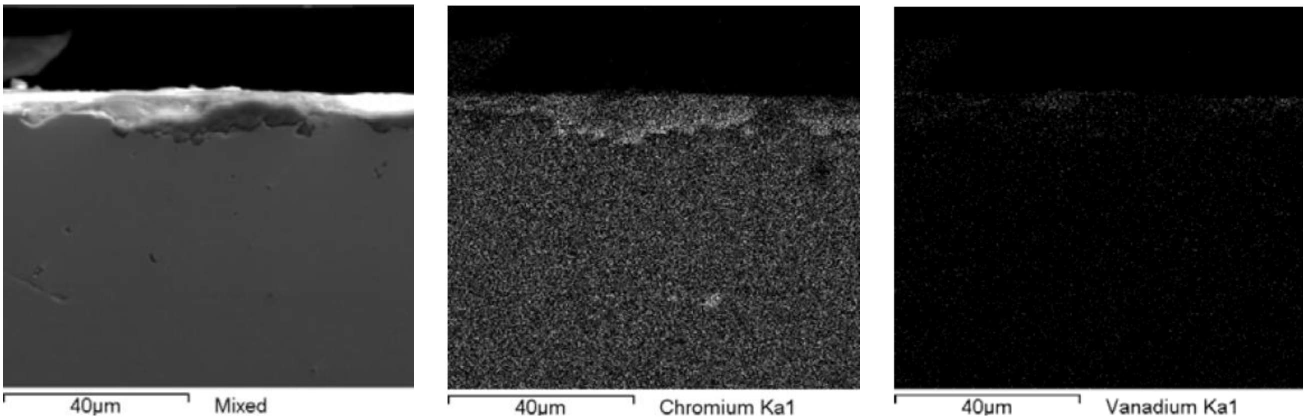

Inconel 617

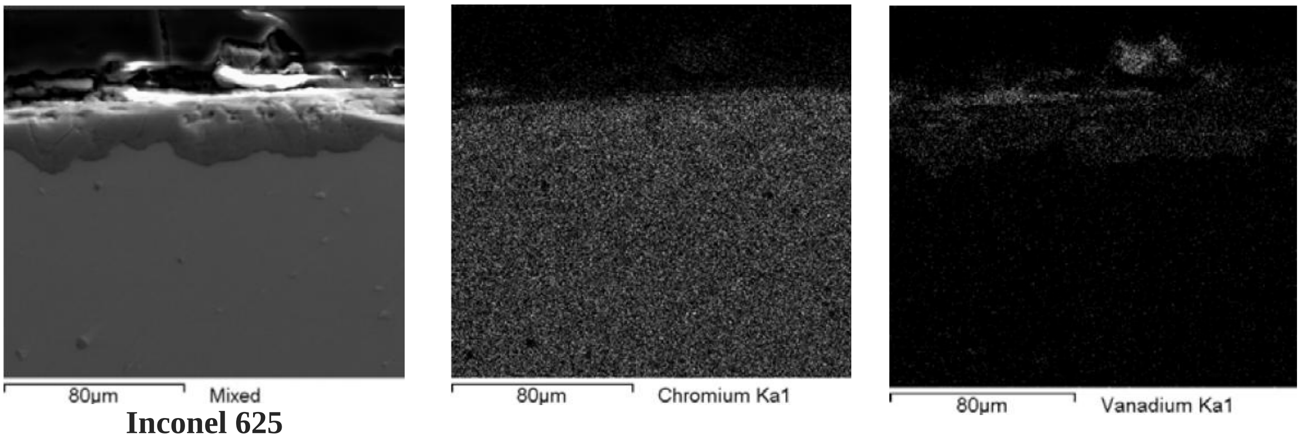

Inconel 625

Figure 10. Micrographs of the metal-scale interface of the Ni-based alloys corroded in $NaVO_3$ for 100 hours at 700 °C together with X-ray mappings for Cr and V.

4. CONCLUSIONS

A study of the corrosion performance of Ni-based alloys (Inconel 600, 601, 617 and 625) in $NaVO_3$ molten salt at 700 °C was realized. In order to determine the corrosion resistance of the alloys, electrochemical techniques and weight loss tests were used. According to results, it was observed that Inconel 600 and 601 showed the best corrosion resistance, however the Inconel 617 and 625 showed a poor performance. This was because these alloys besides the Cr and Ni, they containing other elements, for example, Fe, Mo, Al, Co or Nd-rich and Ti-rich precipitates, which affect the corrosion resistance due to the synergistic dissolution of the different metallic oxides formed and the Nd-rich and Ti-rich precipitates generated anodic-cathodic sites favoring the corrosion of the alloy.

Conflict of Interests

The authors declare that there is no conflict of interests regarding the publication of this paper.

ACKNOWLEDGEMENTS

Financial support from Consejo Nacional de Ciencia y Tecnología (CONACYT, México) (Projects 196205, 159898, and 159913), and Ph.D. scholarship to O. Sotelo-Mazon (registration number 227517) is gratefully acknowledged.

References

1. T.S. Sidhu, S. Prakash, R.D. Agrawal, *Current Science*, 90 (2006) 41.
2. Y. Harada, S. Naito, T. Tsuchiya, Y. Nakajima, Mitsubishi Technical Bulletin 85, 1981.
3. T. Kawamura, Y. Harada, Mitsubishi Technical Bulletin 139, 1980.
4. H.W. Halstead, *Journal of the Institute of Fuel*, 43 (1970) 234.
5. A. Wong-Moreno, R.I. Marchan Salgado, *CORROSION 95*, paper 465, (Houston, TX: NACE Intl. 1995).
6. A. Wong-Moreno, Y. Mujica, L. Martinez. *CORROSION* 94, paper 185, (Houston, TX: NACE Intl. 1994).
7. J. Porcayo-Calderon, V.M. Salinas-Bravo, R.A. Rodriguez-Diaz, L. Martinez-Gomez, *Int. J. Electrochem. Sci.*, 10 (2015) 4928.
8. K. Natesan, *Corrosion*, 32 (1976) 364.
9. J.G. Gonzalez-Rodriguez, S. Haro, A. Martinez-Villafañe, V.M. Salinas-Bravo, J. Porcayo-Calderon, *Materials Science and Engineering A*, 435-436 (2006) 258.
10. H. Singh, D. Puri, S. Prakash, *Reviews on Advanced Materials Science*, 16 (2007) 27.
11. C. Cuevas-Arteaga, J. Uruchurtu-Chavarin, J. Porcayo-Calderon, G. Izquierdo-Montalvo, J. Gonzalez, *Corros. Sci.*, 46 (2004) 2663.
12. C. Cuevas-Arteaga, J. Uruchurtu-Chavarin, J. Gonzalez, G. Izquierdo-Montalvo, J. Porcayo-Calderon, U. Cano-Castillo, *Corrosion*, 60 (2004) 548.
13. P.S. Sidky, M.G. Hocking, *Corros. Sci.*, 27 (1987) 499.
14. N.Q. Minh, B.J. Welch, *Aus. J. Chem.*, 28 (1975) 965.
15. J.I. Barraza-Fierro, M.A. Espinosa-Medina, M. Hernandez-Hernandez, H.B. Liu, E. Sosa-Hernandez, *Corros. Sci.*, 59 (2012) 119.
16. F. H. Stott, J. L. Dawson, D. M. Farrell, *Oxidation of Metals*, 33 (1990) 79.
17. E. Otero, A. Pardo, M. C. Merino, M.V. Utrilla, M.D. Lopez, J.L. del Peso, *Oxidation of Metals*, 51 (1999) 507.
18. E.M. Zahrani, A.M. Alfantazi, *Corros. Sci.*, 65 (2012) 340.
19. E.M. Zahrani, A.M. Alfantazi, *Metallurgical and Materials Transactions A*, 43 (2012) 2857.
20. E.M. Zahrani, A.M. Alfantazi, *Corros. Sci.*, 85 (2014) 60.
21. J. Chen, Z. Huang, Y. Ren, W. Li, W. Qiu, J. Chen, J. He, *High Temperature Materials and Processes*, 32 (2013) 581.
22. Y. Wang, H. Liu, C. Zeng, *Journal of Fluorine Chemistry*, 165 (2014) 1.
23. Y.L. Wang, Q. Wang, H.J. Liu, C.L. Zeng, *RSC Adv.*, 5 (2015) 32755.
24. K.K. Kasem, S. Jones, *Platinum Metals Rev.*, 52 (2008) 100.
25. Y. Longa-Nava, Y.S. Zhang, M. Takemoto, R.A. Rapp, *Corrosion*, 52, (1996) 680.

26. R. Baboian, S. Dean, H. Hack, G. Haynes, J. Scully, D.O. Sprowls, *Corrosion Tests and Standards: Application and Interpretation*, ASTM Manual Series, MNL20, ASTM, Philadelphia PA, USA, 1995.
27. G.M. Lu, S.Z. Shang, J.J. Yu, J.G. Yu, *Applied Mechanics and Materials*, 52-54 (2011) 1538.
28. J. Porcayo-Calderon, O. Sotelo-Mazon, V.M. Salinas-Bravo, C.D. Arrieta-Gonzalez, J.J. Ramos-Hernandez, C. Cuevas-Arteaga, *Int. J. Electrochem. Sci.*, 7 (2012) 1134.
29. G. Salinas-Solano, J. Porcayo-Calderon, J.G. Gonzalez-Rodriguez, V.M. Salinas-Bravo, J.A. Ascencio-Gutierrez, L. Martinez-Gomez, *Advances in Materials Science and Engineering,* 2014 (2014), Article ID 696081, 8 pages.
30. Y.S. Hwang, R.A. Rapp, *Corrosion*, 45 (1989) 933.
31. Y. Longa-Nava, Y.S. Zhang, M. Takemoto, R.A. Rapp, *Corrosion*, 52 (1996) 680.
32. I. Gurrappa, *Surface and Coatings Technology*, 139 (2001) 272.
33. M.C.RA. Rezende, A.P.R. Alves, E.N. Codaro, C.A.M. Dutra, *Mater. Science: Materials in Medicine*, 18 (2007) 149.
34. E.E. Stansbury and R.A. Buchanan, Fundamentals of Electrochemical Corrosion, ASM International, Ohio (2000).
35. T.J. Pan, C.L. Zeng, Y. Niu, *Oxidation of Metals*, 67 (2007) 107.